

Composition–microstructure–property relationships in ceramic monofilaments resulting from the pyrolysis of a polycarbosilane precursor at 800 to 1400 °C

E. BOUILLON, D. MOCAER, J. F. VILLENEUVE, R. PAILLER, R. NASLAIN
*Laboratoire des Composites Thermostructuraux, (UM 47-CNRS-SEP-UB1), Europarc,
3 Avenue Léonard de Vinci, F33600-Pessac, France*

M. MONTHIOUX, A. OBERLIN
*Laboratoire Marcel Mathieu (UA 1205 CNRS), Université de Pau, 2 Avenue du Président Angot,
F64000-Pau, France*

C. GUIMON, G. PFISTER
*Laboratoire de Physico-Chimie Moléculaire (UA 474-CNRS) Université de Pau,
Avenue de l'Université, F64000-Pau, France*

A 15 μm monofilament was extruded from a Yajima's type molten polycarbosilane, stabilized by addition of oxygen and heat-treated at 800 to 1400 °C under an argon atmosphere. Two important phenomena occur during pyrolysis. At 500 to 750 °C, an organic–inorganic state transition takes place with a first weight loss. It yields an amorphous material stable up to about 1100 °C. At this temperature, its composition is close to $\text{Si}_4\text{C}_5\text{O}_2$. It can be described as a continuum of SiC_4 and/or $\text{SiC}_{4-x}\text{O}_x$ tetrahedral species (and possibly contains free carbon), with a homogeneity domain size less than 1 nm. The amorphous filament exhibits a high strength and semi-conducting properties. Above 1200 °C, a thermal decomposition of the amorphous material takes place with an evolution of gaseous species thought to be mainly SiO and CO, an important cross-section shrinkage and the formation of 7 to 20 nm SiC crystals which are surrounded with a poorly organized turbostratic carbon. The amorphous–crystalline state transition results in a drop in the tensile failure strength and an increase, by four orders of magnitude, in the electrical conductivity which becomes temperature independent. The former effect is due to the crystallization of the filament and the latter to a percolation phenomenon related to the intergranular carbon. The low stiffness is also due to the presence of carbon. It is anticipated that this transition is mainly related to the decomposition of the silicon oxycarbide species. Finally, a 40 to 50 nm layer of turbostratic carbon is formed at the filament surface at 1200 to 1400 °C whose origin remains uncertain. It is thought to be mainly responsible for the formation of the carbon interphase in the high-temperature processing of ceramic matrix composites.

1. Introduction

Ceramic matrix composites (CMCs) belong to a new family of ceramic materials that could be used extensively by the designers, in a near future, for structural parts submitted to severe environmental conditions (e.g. in high-temperature gas turbines and reciprocating engines, as well as reusable heat shields). With respect to monolithic ceramics, the main advantage of CMCs lies in their high toughness and reliability.

The applications of CMCs are still limited by processing considerations and availability of high-performance ceramic fibres. Recent progress has been made in the field of CMC processing. The chemical vapour infiltration process (used for SiC matrix composites) and the slurry impregnation/hot-pressing

process (used for glass or glass–ceramic matrix composites) are examples of techniques which are already utilized in industry. On the contrary, in the field of ceramic fibres, the progress has been very slow during the last two decades, carbon fibres remaining, in fact, the best reinforcement on the basis of their excellent mechanical properties at high temperatures and low density. Unfortunately, the strong affinity of carbon for oxygen, even at moderate temperatures, precludes the use of CMCs reinforced with carbon fibres in atmospheres containing oxygen unless a protective coating is applied on the fibres and/or the composites [1].

SiC-based fibres, obtained by pyrolysis of a polycarbosilane precursor, were first proposed by Yajima

and co-workers [2–8]. They were prepared according to a procedure very similar to that already used for carbon fibres including the following main steps: (i) spinning of the precursor in the molten state, (ii) cross-linking by oxygen to make the green fibre infusible, and (iii) pyrolysis under an inert atmosphere. Different products derived from Yajima's route are now available on the market, the most common being the Nicalon fibres (NLP 101 and NLM 202, Nippon Carbon). From a chemical point of view, they all belong to the ternary Si–C–O or quaternary Si–C–N–O systems (and even to more complex systems involving, for example, titanium) and are obtained by pyrolysis of polycarbosilane (PCS) or polycarbosilazane (PCSZ) precursors [9–12]. It is worthy of note that the properties of these ceramic fibres have not been significantly improved, in terms of mechanical and thermal stability, with respect to those of the original Yajima ex-PCS fibre despite significant research efforts. This might be the result of two contradictory considerations: (i) a high failure strength in ex-PCS fibres is thought to be related to an amorphous (or at least poorly crystallized) microstructure, whereas (ii) such a microstructure is not stable at high temperatures and tends to crystallize and coarsen with a dramatic drop in failure strength.

According to chemical analysis data, there is both an excess of carbon (with respect to the SiC stoichiometry) and significant amount of oxygen (resulting mainly from the cross-linking step) in ex-PCS fibres. However, the nature of the forms under which this carbon excess and oxygen are present in the fibres is still a matter of controversy and seems to differ from fibre to fibre. Microcrystals of free carbon have been observed by transmission electron microscopy (TEM) in the Nicalon NLM 202 ceramic-grade fibre, but not in the NLP 101 grade, by Maniette and Oberlin [13]. Oxygen was first assumed to be present as silica whereas recent analyses support the occurrence of an amorphous Si(C,O) ternary phase [14, 15]. The state of crystallization of the SiC phase is also different in the two Nicalon fibres, the NLM 202 grade being usually considered to be more crystallized than the NLP 101 grade. Finally, a model of microstructure has recently been proposed by Laffon *et al.* [16] in which the ex-PCS fibre could be described as a nanoscale mixture of SiC and carbon embedded in an Si(C,O) amorphous matrix.

The thermal stability of ex-PCS fibres is an important property because any coarsening of the initial fine-grained microstructure resulting from a heat treatment may lead to (i) an important decrease in the fibre failure strength, as already mentioned and (ii) a change in the composition of the fibre surface modifying the fibre/matrix coupling when it takes place within a composite. This latter effect is thought to be at least partly responsible for the formation of the carbon-based interphase during the high-temperature fabrication of most ex-PCS reinforced CMCs (e.g. SiC (Nicalon)/glass–ceramic composites) and thus for their high toughness [17–22].

As far as the strength of CMCs (which by their nature are intended to withstand long exposures at

high temperatures) is concerned, ex-PCS fibres should have a high thermal stability, whereas recent studies have shown that they undergo important chemical and microstructural changes above about 1100 °C (i.e. far below the peritectic decomposition of SiC at about 2500 °C) [23]. Luthra [24] has shown, from thermodynamic studies, that ex-PCS fibres are intrinsically unstable at high temperatures, their evolution towards equilibrium giving rise to the formation of carbon monoxide as the main gaseous species. On the other hand, Johnson *et al.* [25] have established, on the basis of their Knudsen cell/mass spectrometry data, that the main gaseous species actually formed during heat treatments of ex-PCS fibres under nitrogen up to 1400 °C is silicon monoxide. These gaseous species could result from the thermal decomposition of the ternary Si(C, O) amorphous matrix and could explain (i) the formation of free carbon in the bulk at high temperatures, mentioned by several authors, and (ii) the coarsening of the SiC grains (the SiC grains being less and less isolated by the Si(C, O) continuum as it is progressively destroyed in the Laffon *et al.* model [16]). However, many details of the mechanism of the ex-PCS evolution at high temperatures remain unknown as well as the relations between this evolution and that of the mechanical properties.

Within the frame of a programme of research on ex-PCS ceramics, we have already studied the organic/ceramic transition that occurs during the pyrolysis of bulk PCS and PCSZ precursors including a Yajima's-type PCS and various models [26, 27]. We have now spun, with a single spinneret laboratory-scale apparatus, a Yajima's-type PCS. The aim of the present contribution is to draw a tentative correlation between the thermal variations of the chemical and microstructural features of the ex-PCS ceramic monofilament, on the one hand, and those of its mechanical properties, on the other, as a function of the pyrolysis temperature.

2. Experimental procedure

2.1. Preparation of the ex-PCS ceramic monofilaments

The PCS precursor used in this study (Shinetsu, Japan), was thought to have been prepared according to the Yajima's route, i.e. by thermal treatment in an autoclave of polydimethylsilane [5]. In a first approximation, its theoretical formula is $-(\text{HSiCH}_3-\text{CH}_2)_n-$. The as-received product was slightly modified (M_n adjusted to 1500) in order to allow its spinning in the molten state.

The PCS precursor was spun, at a temperature of about 300 °C, as a continuous monofilament, 10 to 15 μm diameter, with a single spinneret laboratory-scale apparatus, under an atmosphere of dry nitrogen. The green filament was then cut into lengths of about 50 mm and rendered infusible by oxygen cross-linking at about 160 °C. Finally, the pyrolysis treatments of the stabilized samples were performed, under a flow of dry argon, at temperatures ranging from 600 to 1400 °C according to a procedure which has been described elsewhere [26].

2.2. Chemical analyses

Thermogravimetric analysis (TGA, SETARAM TAG 24) was performed under an atmosphere of dry argon, according to a heating temperature/time curve similar to that used for the preparation of the monofilaments.

The element analysis (for silicon, carbon and oxygen) was performed (CAMEBAX 75), on monofilament cross-sections, by electron probe microanalysis (EPMA) in the wavelength dispersion mode (the curved analysers being PET for $\text{SiK}\alpha$ and multi-layered PCI for both $\text{CK}\alpha$ and $\text{OK}\alpha$). The method was validated on cross-sections of NLM 202 Nicalon fibres whose chemical composition has been assessed independently by conventional chemical analysis.

The XPS spectra were recorded (SSI/301 XPS spectrometer) with $\text{AlK}\alpha$ (1486.6 eV) as the excitation source, on filament tows, the irradiated surface of the material having a width of about 600 μm and a length of 700 μm . The analyses were performed, under a residual pressure less than 5×10^{-8} Pa, on as-spun filaments, after the oxygen cross-linking step, as well as after pyrolysis at 600, 700 and 850 °C. Because all the materials were insulators, the charge effect was compensated with an electron flood gun, the energy of the electrons (in the 2 to 10 eV range) being adjusted with respect to the nature of the material. If the green PCS filament sample whose stability was not high enough is disregarded, all the samples were cleaned by Ar^+ ion bombardment (10 mA intensity, 4 kV energy) prior to XPS analysis, as follows: (i) 10 min exposure for all samples, and (ii) additional 1, 20 and 30 min exposures for the samples heat treated at 850 °C. Before applying this cleaning treatment, the sample surface was found to be contaminated with carbon (C 1s peak at 184.6 eV; 1 to 8 at. %). Finally, the XPS data recorded on the heat-treated PCS samples were calibrated utilizing the C 1s binding energy in SiC (283.3 eV as a standard).

Auger electron analyses were performed with an AES microanalyser (Perkin-Elmer PH1-590 SAM) according to the depth-profiling mode. The spectra were recorded from the heat-treated filament surfaces (spot size of about 1 μm) which were progressively etched with an Ar^+ ion gun. The intensities of selected Auger electron transitions (i.e. *LVV* for silicon, *KLL* for carbon, and *KLL* for oxygen) were recorded as a function of the thickness of material which has been sputtered.

2.3. Nano- and microstructural analyses

The nano- and microstructural features of the heat-treated PCS monofilaments were derived from TEM analyses (Philips EM 400). The thin foils were prepared according to the following procedure: (i) the ex-PCS monofilaments were first embedded in an epoxy resin, (ii) after curing and shaping, the block of resin was cut into thin foils (less than 50 nm thick) with an ultramicrotome. The thin foils were set on a copper microgrid coated with a thin film of amorphous carbon (less than 10 nm) and introduced into the high-resolution microscope.

The apparent diameter of the aperture in the Abbe plan of the objective lens of the microscope was

(i) 2 nm⁻¹ in the dark-field imaging mode, and (ii) 8.2 nm⁻¹ in the lattice-fringe imaging mode. The selective dark-field images were obtained by exploring radially and azimuthally the reciprocal space, according to a technique which has been described elsewhere [28, 29]. Two aperture positions were used: in position 1, the aperture is centred at 2.4 nm⁻¹ and its diameter admits, among others, the 002 reflection of carbon (and possibly the most intense halo of amorphous SiO_2), whereas in position 2, it is centred at 4.2 nm⁻¹ and selects among others the 111 reflection of β -SiC.

2.4. Electrical conductivity

The electrical conductivity was measured up to 530 °C under an atmosphere of helium. The measurements were performed on ten monofilament tow sets on alumina plates, the electrical contacts being secured with a silver lake.

2.5. Mechanical tests

Both tensile and torsion tests were performed at room temperature, on the ex-PCS monofilaments, in order to derive the elastic Young's and shear moduli as well as the ultimate tensile stress.

The tensile tests were performed with an apparatus similar to that used by Bunsell *et al.* [30]. The applied load was measured with a strain sensor directly connected to the grip, whereas the strain was measured with a classical differential strain sensor fastened on the ram. The method was validated on Nicalon NLM 202 monofilaments, the data, i.e. $E = 210$ GPa and $\sigma^R = 2500$ MPa (gauge length 10 mm), being consistent with those generally given for this material.

The torsion tests were performed with an original apparatus which will be described in detail elsewhere [31]. In principle, the apparatus is a micropendulum utilizing the monofilament as torsion wire. The monofilament is fastened at one end to the axis of a d.c. motor (which is used to load the monofilament in torsion) and, at the other end, to an inertial disc printed with angular sectors alternately black and white. After having been loaded in torsion, the pendulum is allowed to oscillate freely, the oscillations being recorded with an opto-electronic infrared sensor acting directly on the black/white inertia disc. The shear modulus was derived from the period of the oscillations assuming that the material is isotropic. The shear modulus of the Nicalon NLM 202 filaments, measured according to this technique was 76 ± 5 GPa, a value which agrees well with that given by the fibre producer (i.e. 77 GPa).

Finally, the monofilament diameters were measured by laser interferometry.

3. Results and discussion

3.1. Chemical change during PCS filament pyrolysis

3.1.1. TGA observations

As shown in Fig. 1, the TGA curve of a spun PCS sample, performed after the oxygen cross-linking step,

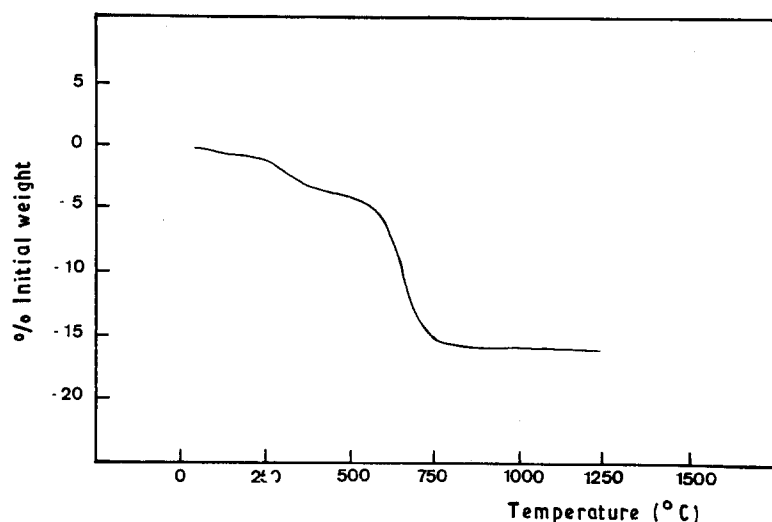


Figure 1 Weight loss occurring during the pyrolysis under an inert atmosphere of PCS filaments previously cross-linked by oxygen, as a function of temperature.

suggests that two important transitions occur in the material as temperature is increased, at 500 to 750 °C and above about 1100 to 1200 °C. The former results in a weight loss of 10% and is thought to correspond to the breaking of most organic bonds with the formation of gaseous species (i.e. hydrocarbons and possibly silicon-based organometallic species), as previously observed during the bulk pyrolysis of the same PCS [26]. It is worthy of note that some weight loss (of the order of 4%) has already occurred before the organic-inorganic transition (i.e. at about 250 °C) which may be assigned to an evolution of polycarbosilanes of low molecular weights (either present in the material or formed during the very first steps of the pyrolysis). The latter transition takes place at higher temperatures, i.e. between 1200 and 1400 °C (average diameter changes from 16 μm to less than 13 μm). It results in a marked decrease in the oxygen content of the fibre (from 20% to 2%) and to some decrease in its silicon content (which falls from 35% to 30%), as shown in Table I.

The first stages of the pyrolysis of stabilized PCS filaments (at $T < 1000$ °C) exhibit, compared to those reported by Bouillon *et al.* [26] for unstabilized PCS bulk samples of same origin, the following main differences: (i) the weight loss is greatly limited (i.e. about 16% instead of 40%), and (ii) the organic-inorganic transition starts at a higher temperature (i.e. about 500 °C instead of 350 °C). These differences may have two origins. On the one hand, part of the low molecular weight polycarbosilanes which are responsible for the important weight loss occurring in bulk PCS at

low temperatures (300 to 400 °C), has been eliminated from the PCS precursor before filament spinning. On the other hand, the Si-O-Si chemical bonds (and probably some C-Si-O bonds) formed during the stabilization of the green PCS filament, are strong bonds which increase the thermal stability of the material.

These conclusions agree with those previously drawn by Poupeau *et al.* [32] or Hasegawa and Okamura [10] from analyses performed during the pyrolysis of bulk or green fibre samples.

3.1.2. XPS and EPMA derivations

XPS analyses performed at different stages of PCS-filament pyrolysis show that all materials are made of silicon (Si2s and Si2p peaks), carbon (C1s peak) and oxygen (O1s peak), as illustrated in Fig. 2 for the pyrolytic residue obtained at 850 °C. Hydrogen, if present, which is actually the case for $T_p < 850$ °C, was not analysed, as already mentioned. The energy values corresponding to the various chemical bonds, derived from the XPS peaks (recorded in the high-resolution mode) are listed in Table II.

The C 1s peak consists of two components (Fig. 3a). The first (I) at 283.3 eV, assigned to C-(Si)_x bonds, and the second (II) between 284.2 and 284.4 eV, assigned to C-C and perhaps to C-(Si)_y bonds ($y < x$), are present in the spectra of both the polymeric and ceramic materials. Finally, a third component (III), beyond 285 eV, is also observed after the cross-linking step, its intensity decreasing as T_p is raised (Fig. 3b). This latter component, already mentioned by Porte and Sartre in their study on Nicalon fibres disappears after sputtering and so could be assigned to superficial carbon atoms in an electronegative environment (e.g. that of oxygen) [33].

The Si 2p peak consists of two or three components (Fig. 4). The first (I) at about 101 eV is assigned to Si-C bonds whereas the second (II) at about 103.2 eV (Fig. 4a), only observed in the spectra recorded near the surface of filaments treated at 850 °C, has been assigned to Si-O bonds similar to those present in silica [34]. Finally, a third component (III) at 102.3 eV for the polymeric materials and which is shifted to 101.9 eV as pyrolysis proceeds towards the ceramic

TABLE I EPMA chemical analyses of PCS filaments after oxygen cross-linking and pyrolysis at increasing temperatures. The atomic percentages given for $T_p = 850$ °C do not take into account hydrogen (thought to be still present in significant amounts at this temperature). The data for NICALON NLM-202 (obtained at about 1200 °C) are given for comparison

Materials	Si (at. %)	C (at. %)	O (at. %)
Nicalon NLM-202	38	49	13
PCS-filaments			
heated at: 850 °C	35	44	20
1200 °C	36	44	19
1400 °C	30	67	2

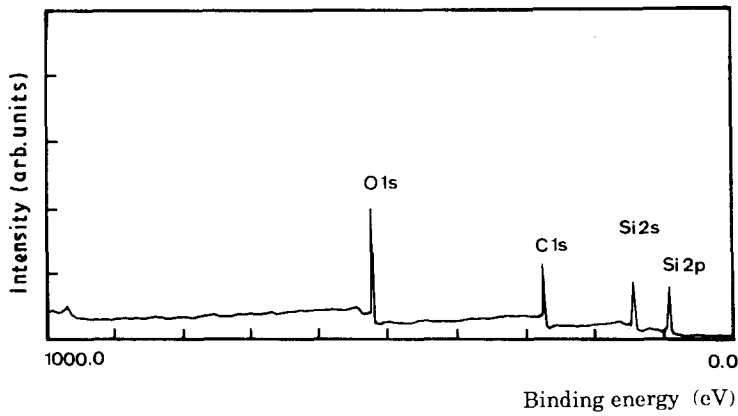


Figure 2 XPS spectrum of PCS filaments stabilized by oxidation and heat treated at 850°C under an inert atmosphere (recorded after 30 min of Ar⁺ ion sputtering).

TABLE II Binding energies (eV) derived, from the XPS peaks in untreated, cross-linked and heat treated PCS

Filament treatment	Ar ⁺ ion etching	C 1s peak			Si 2p peak		
		C-Si(I)	C-Si(II)	C-O(III)	Si-C(I)	Si(C, O)(III)	Si-O(II)
Before cross-linking	none	283.3	284.4	—	101.0	—	—
After cross-linking	none	283.3	284.3	285.3	100.9	102.0	—
After cross-linking	10 min	283.3	284.5	—	100.7	101.9	—
At 600°C	none	283.3	284.5	285.5	101.1	102.3	—
At 600°C	10 min	283.3	284.3	285.2	100.9	102.3	—
At 700°C	none	283.3	284.4	285.4	101.3	102.5	—
At 700°C	10 min	283.3	284.3	285.3	101.0	102.3	—
At 800°C	1 min	283.3	284.2	285.2	101.1	102.1	103.2
At 800°C	10 min	283.3	284.2	—	100.8	101.9	—
At 800°C	30 min	283.3	284.2	—	100.8	101.9	—

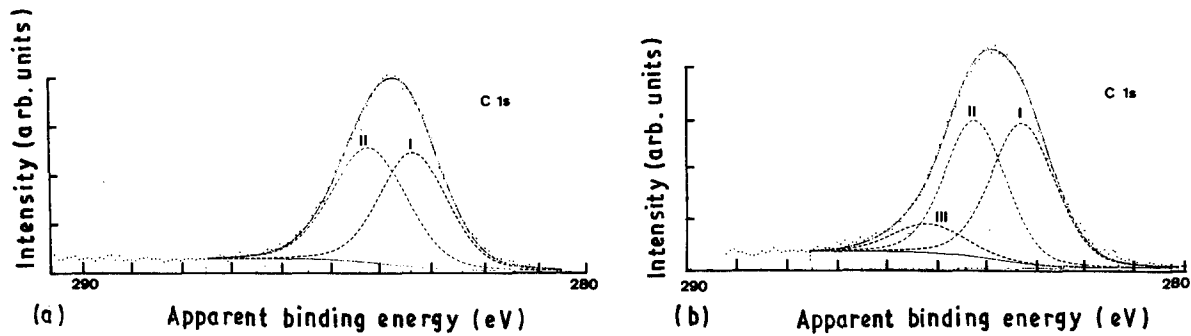


Figure 3 Decomposition of the C 1s peaks of the XPS high-resolution spectra of PCS filaments stabilized with oxygen and heat treated under an inert atmosphere at (a) 850°C (Ar⁺ etching 30 min), and (b) 600°C (Ar⁺ etching 10 min).

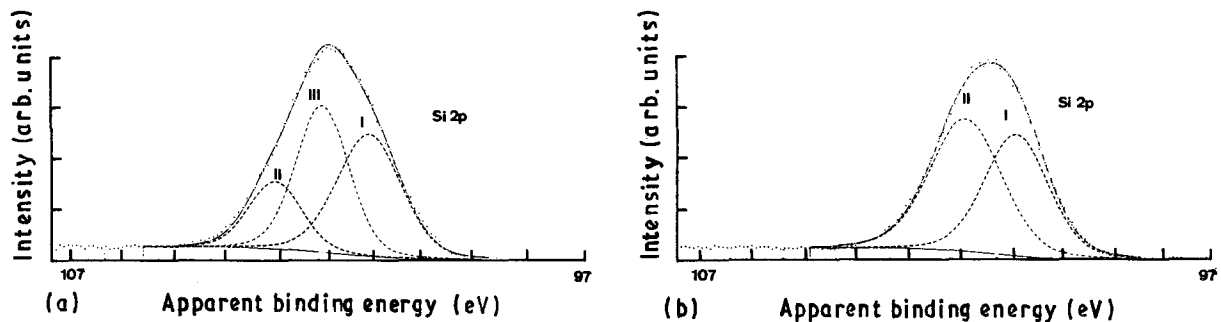


Figure 4 Decomposition of the Si 2p peaks of the XPS high-resolution spectra of PCS filaments stabilized with oxygen and heat treated under an inert atmosphere at 850°C. The spectra were recorded after Ar⁺ etching for (a) 1 min and (b) 30 min.

state, is also observed between those corresponding to Si-C and Si-O bonds. It is assigned to a ternary Si(C,O) species. A similar component (at 101.5 eV) has also been recently reported for Nicalon fibres [33].

A shift of the Si 2p binding energy towards the low energies is observed after sputtering. This fact, already

observed by Mizokawa *et al.* [35] could be due to a preferential sputtering of the carbon of SiC and thus to the formation of a silicon-rich surface with possibly Si-Si bonds.

Our XPS data recorded from PCS filaments, cross-linked by oxygen and heat-treated under an inert

atmosphere at 850 °C, confirm the complex chemical nature of different ex-organosilicon precursor fibres, which has been already mentioned by several authors [14, 16, 33]. In order to ascertain the assignments of the XPS peak components to chemical bonds, our data are compared in Table III with data available from literature for silicon-based materials. The binding energies derived from components I of C 1s and Si 2p peaks are very close to those reported for CVD β -SiC [35]. The binding energy derived from component II of the C 1s peak can be assigned to C–C and C–Si bonds. The binding energy, corresponding to component II of the Si 2p peak assigned to Si–O bonds, is similar to that mentioned for silica. Finally, component III of the Si 2p peak was assigned to a ternary Si–(C,O) species as already proposed by Porte and Sartre in their XPS study of Nicalon fibres [33]. Such a ternary Si–(C,O) species, sometimes referred to as Si–X, was also mentioned earlier by Sawyer *et al.* [15] or Lipowitz *et al.* [14]. Because this component Si 2p (III) is already present in the XPS spectrum of the cross-linked PCS (Table II), one could assume that the formation of the Si(C, O) bonding occurs during the stabilization of the green PCS fila-

ment by oxygen. On the other hand, the thin silica layer (thickness less than 5 nm) present at the filament surface for $T_p = 850$ °C and which is responsible for component II of the Si 2p peak (Fig. 4a), is probably due to an oxidation by trace amounts of residual oxygen in the pyrolysis furnace atmosphere, during and after the organic–ceramic transition.

A quantitative analysis of the chemical bonds in the materials at different steps of the filament processing is given in Table IV. It appears that the initial PCS precursor (i) is almost free of oxygen, and (ii) shows at least two different carbons corresponding to two bonds. However, part of these C–C bonds could also be due to contamination by carbon (because no surface etching has been done prior to XPS analysis as already mentioned). The data also show that a large amount of oxygen is introduced in the PCS during the stabilization step and not removed during the organic–ceramic transition at 500 to 750 °C. Because an important weight loss occurs during this transition, the pyrolytic residue at 850 °C still contains a higher percentage of oxygen. Finally, during the transition, the percentage of silicon remains almost constant, whereas that of carbon regularly decreases. This result

TABLE III Binding energies (eV) corresponding to different atomic bondings in various materials containing silicon

Materials	Si 2p peak			C 1s peak			References
	Si–C (I)	Si–(C, O) (III)	Si–O (II)	C–Si (I)	C–Si (II)	C–O (III)	
Si _{1-x} C _x :H films (glow discharge)	100.0			283.0	284.1		[38]
CVD SiC	101.2		103.4	283.2			[35]
CVD SiC and graphite	100.5			282.7	284.3		[37]
SiO ₂ -layer on silicon	101.1	102.2	103.2	283.3	284.3	284.9	[34]
Oxidized polycrystalline SiC	100.5		103.1				[36]
Oxidized SiC	100.2		103.1	282.3		284.8	[39]
Nicalon fibres surface	100.5	101.5	103.2	283.3	284.9		[33]
Bulk	100.5	101.5	103.1	283.3	284.6	285.6	
ex-PCS filament surface	101.1	102.2	103.2	283.3	284.3	284.9	Present
Bulk	100.8	101.9		283.3	284.2		work

TABLE IV Quantitative XPS analysis of the chemical bonds (at. %) at different steps of the organic–ceramic transition of a PCS precursor

Materials	Ar ⁺ etching time (min)	C 1s peak			Si 2p peak			O 1s peak
		C–Si(I)	C–Si(II)	C–O	Si–C	Si–(C, O)	Si–O	
Before cross linking*	none	28	(65) 37	–	33	(33) –	–	3
After cross linking	10	25	(50) 25	–	21	(32) 11	–	18
Treated at 600 °C	10	22	(47) 20	5	25	(33) 8	–	18
Treated at 700 °C	10	18	(39) 16	5	18	(34) 16	–	27
Treated at 850 °C	1	12	(35) 16	7	13	(32) 13	6	33
	10	18	(37) 19	–	17	(36) 19	–	27
	30	18	(38) 20	–	16	(36) 20	–	26

* The analysis does not take into account hydrogen.

In each case, data given in parentheses correspond to the overall elemental percentages.

TABLE V Chemical analyses of ex-PCS fibrous materials

Materials		Si (at. %)	C (at. %)	O (at. %)
PCS monofilaments	XPS*	36	38	26
heat treated at 850 °C	EPMA*	35	44	20
ex-PCS fibres obtained at ~ 1250 °C [39]		37	40	23

*Hydrogen probably present in small amount, not analysed.

suggests that the gaseous species which are formed during the organic-ceramic transition are mainly carbon-based organic molecules and not silicon-based organometallic molecules, in agreement with the results of gas analyses reported by several authors [7, 8].

The results of the XPS quantitative analysis performed on the filaments heat-treated at 850 °C are compared in Table V with those obtained by EPMA on cross-sections of the same filaments. The agreement is good for silicon but rather poor for both carbon and oxygen. This discrepancy, which has already been observed by Bouillon *et al.* [26] in their study of the pyrolysis of bulk PCS, could be due to a preferential sputtering of carbon and to a reoxidation during the data acquisition at about 5×10^{-8} Pa background pressure as reported by Mizokawa *et al.* [35]. Finally, on the basis of EPMA bulk analysis, it appears that the chemical composition of our ex-PCS monofilaments is close to that reported by Yajima *et al.* for their first generation ex-PCS fibres [40].

The variations of the chemical composition of the filaments, calculated from XPS data for $T_p < 850$ °C and EPMA data for $T_p > 850$ °C, are shown in Fig. 5 as a function of the temperature of pyrolysis. Two temperature domains correspond to an important change in the chemical composition of the filaments: (i) $500 < T_p < 750$ °C, and (ii) $T_p > 1200$ °C. The former is related to the organic-ceramic transition and the latter is thought to be associated with the thermal decomposition of the Si(C,O) amorphous phase with an evolution of gaseous spe-

cies. The strong increase in the C/Si ratio, observed for $T_p > 1200$ °C, suggests that oxygen might be preferentially removed as SiO (rather than as CO), a result which is in agreement with the conclusions of the study of Johnson *et al.* [25] based on Knudsen cell/mass spectrometer experiments.

3.2. Structural and microstructural change during PCS filament pyrolysis

3.2.1. TEM observations

PCS filaments, cross-linked by oxygen and heat treated at 1100 to 1200 °C under an inert atmosphere, appear as amorphous materials on the basis of their electron diffraction patterns which consist of very broad rings, as shown in Fig. 6a. This result is corroborated by the facts that (i) the bright-field image shows a very smooth microstructure (Fig. 7), and (ii) the radial analysis of the reciprocal space yields dark-field images which consist of faint dots distributed uniformly and whose mean size, i.e. less than 1 nm, is at the limit of resolution of the microscope (Fig. 8a and c). However, it cannot be ascertained that free carbon was not already present in the bulk of the fibre for this low T_p value, as isolated basic structural units (BSUs), i.e. as turbostratic stacks of two or three aromatic layers of about ten aromatic carbon cycles [41, 42]. In fact, such isolated BSUs would give, in dark-field imaging, dots of about 1 nm. On the contrary, free carbon is clearly observed, at the fibre surface as a layer whose thickness is of the order of 5 nm (arrows in Fig. 8a). In this layer, the carbon BSUs are almost parallel to each other and to the fibre surface because this layer is no longer bright when the aperture is moved in a position located in a perpendicular direction (Fig. 8b).

When heat-treated at 1400 °C, the ex-PCS filaments are well crystallized as shown by the electron diffraction pattern which consists of the narrow diffraction rings of β -SiC (Fig. 6b). The crystalline character of the material is also evident from the bright-field image which shows (i) a polycrystalline microstructure in

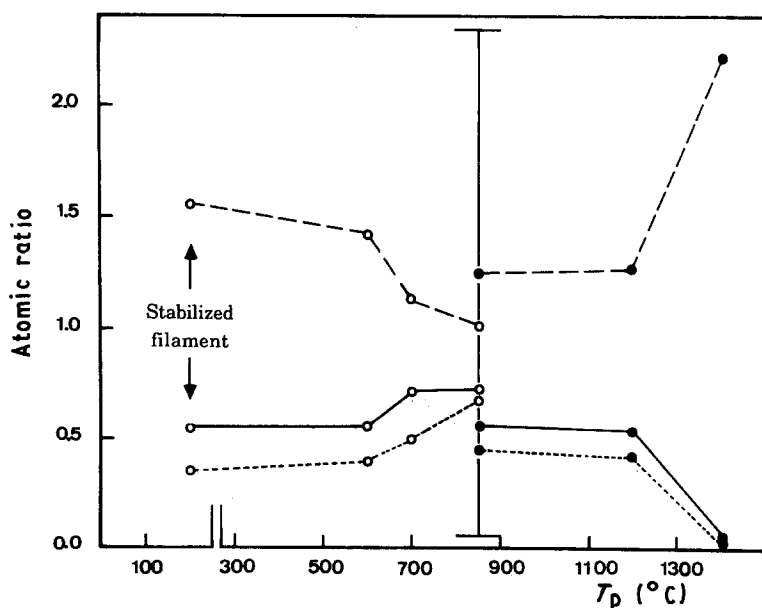


Figure 5 Variations of the (---) C/Si; (—) O/Si and (----) O/C atomic ratios in ex-PCS filaments as a function of the pyrolysis temperature T_p , calculated from the XPS data for $T_p < 850$ °C and EPMA data beyond 850 °C.

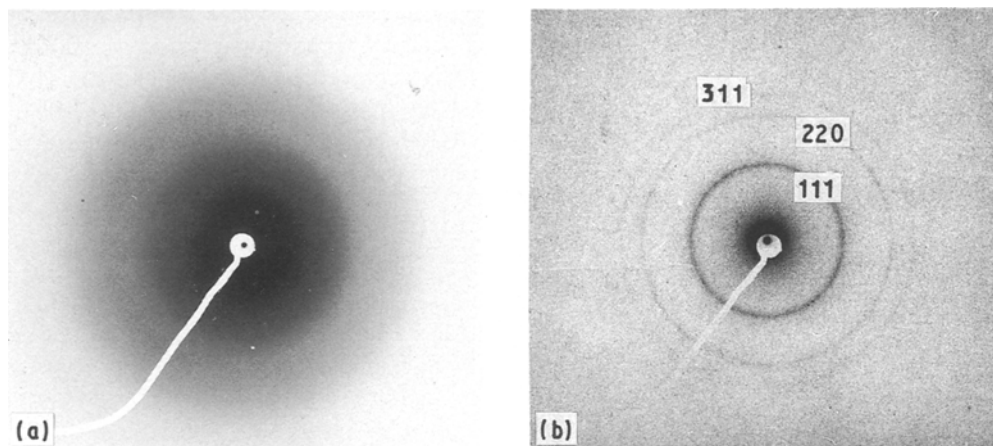


Figure 6 Electron diffraction patterns of PCS filaments stabilized with oxygen and heat treated under an inert atmosphere at (a) 1100 to 1200 °C, and (b) 1400 °C.

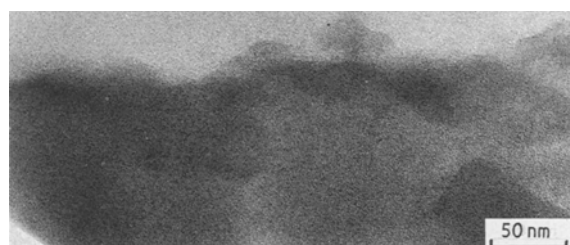


Figure 7 TEM analysis of a PCS filament stabilized with oxygen and heat treated at 1100 to 1200 °C under an inert atmosphere: bright-field image.

the bulk, with a mean SiC grain size of about 7 nm (a few crystals having a size as large as 20 nm), and (ii) a layer with a different microtexture near the filament surface (arrow) and whose thickness is about 40 nm (Fig. 9). This layer consists only of carbon because it is, respectively, bright or dark when the aperture is moved from position 1 to position 2 (see Section 2.3) in dark-field imaging (Fig. 10a and c). Amorphous silica, in which the specific TEM features are not found, is excluded (texture in bright-field mode, brightness of dots in dark-field mode). Moreover, the carbon BSUs do not have any preferential orientation within this layer because the dark-field images are statistically identical when the aperture in position 1 is located in two perpendicular directions (Fig. 10a and b). This 40 nm carbon skin is itself coated with a rim of turbostratic carbon (5 to 7 nm thick) whose aromatic sheets are both parallel to each other and to the filament surface (because it appears bright in Fig. 10a, arrowed, and dark in Fig. 10b). The carbon dark-field images also show the occurrence of faint bright dots in the bulk of the fibre, which correspond to carbon BSUs. This carbon, surrounding the SiC microcrystals is more poorly organized than that from the 40 nm thick carbon layer at the filament surface. This latter feature is clearly apparent from the lattice fringe image shown in Fig. 11. In this picture, the carbon BSUs in the 40 nm thick carbon skin (small arrows) which are associated to form a porous texture as well as those from the 5 to 7 nm thick carbon rim (double arrows) are clearly apparent whereas the carbon BSUs surrounding each SiC crystal (thick arrow)

are hardly seen. This fact (i.e. the degradation of the internal carbon) was recently demonstrated as systematically coming with the drastic SiC crystal growth in Nicalon fibres at high temperatures [43].

Surprisingly, the degradation of free carbon is not observed in the 1400 °C heat-treated bulk (uncured PCS) [26, 29].

3.2.2. AES observations

The AES depth composition profiles, shown in Fig. 12 for $T_p = 1200$ and 1400 °C, are in the main in agreement with the conclusions drawn above from the XPS and TEM analyses.

Carbon in excess is observed near the filament surface as a film which is very thin for $T_p = 1200$ °C and much thicker for $T_p = 1400$ °C. Below this carbon layer, the percentages of both silicon and carbon fall to constant values, very rapidly for $T_p = 1200$ °C and more slowly for $T_p = 1400$ °C, a feature which suggests that the accumulation of carbon near the filament surface might result from a diffusion rate-controlled mechanism.

It is worthy of note that the oxygen concentration is almost nil in the filament heat-treated at 1400 °C (as already established from the XPS and EPMA data) whereas it is very large in that heat-treated at 1200 °C, a feature which confirms that the important structural/microstructural change which occurs in the 1200 to 1400 °C temperature range is related to a chemical mechanism involving the evolution of oxygen-containing gaseous species (e.g. the thermal decomposition of the ternary Si(C, O) species).

3.3. Electrical conductivity change during PCS filament pyrolysis

The results of the electrical conductivity measurements, performed on PCS filaments, first cross-linked by oxygen addition and then heat-treated at increasing T_p (with $T_p = 850, 1100, 1200$ and 1400 °C), are shown in Fig. 13. Generally speaking, the electrical conductivity measured at a given temperature, T_m , increases first slowly for $850 < T_p < 1200$ °C and then

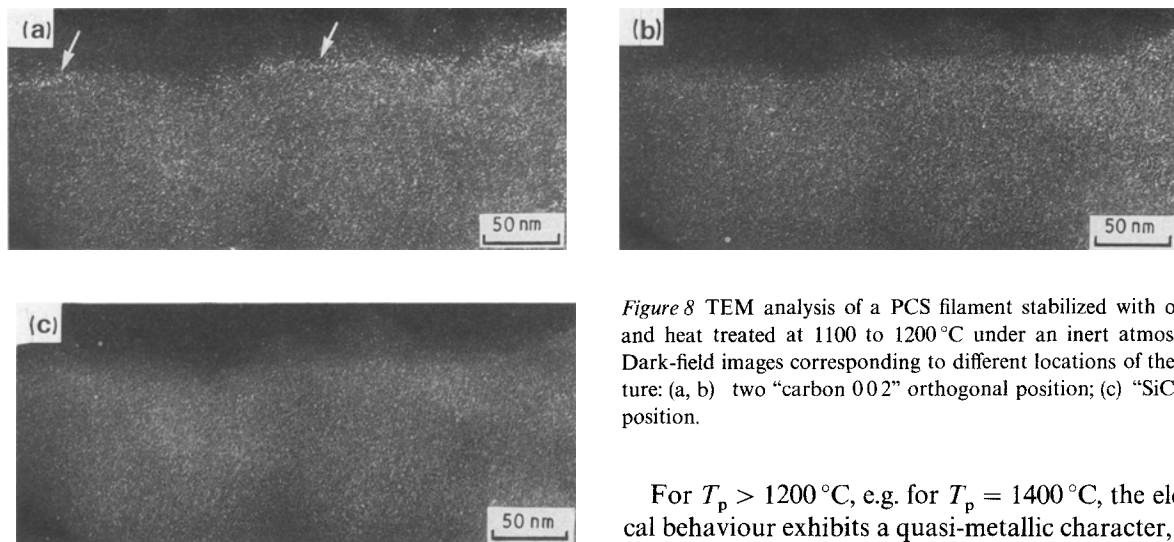


Figure 8 TEM analysis of a PCS filament stabilized with oxygen and heat treated at 1100 to 1200 °C under an inert atmosphere. Dark-field images corresponding to different locations of the aperture: (a, b) two “carbon 002” orthogonal position; (c) “SiC 111” position.

dramatically above 1200 °C, i.e. by almost four orders of magnitude when T_p is raised from 1200 to 1400 °C.

For $T_p < 1200$ °C, the electrical behaviour of the heat-treated PCS filaments is very similar to that previously reported for the solid residues resulting from the pyrolysis (up to about 1000 °C) of the same PCS performed without the cross-linking step on bulk samples [26]. The main features of the $\ln \sigma = f(T^{-1})$ suggest two conduction mechanisms which are successively predominant as temperature is raised. At low temperatures (for $T_m < 320$ °C), the thermal variations of the electrical conductivity are very limited and could be related to a saturation phenomenon in which the electrical conductivity is due to carriers whose number is almost independent of temperature. Such a conductivity could be associated with the C–C bonds from aromatic cycles still containing some hydrogen atoms. At high temperatures ($T_m > 320$ °C), the electrical conductivity is thermally activated with an activation energy of the order of 0.4 eV, a value which falls between those characterizing SiC single crystals ($\Delta E = 0.3$ eV) and polycrystalline SiC ($\Delta E = 0.6$ eV). However, it should be mentioned that no crystalline SiC has been observed for $T_p < 1200$ °C on the basis of TEM analyses. Therefore, the high-temperature part of the $\ln \sigma = f(T^{-1})$ curve might be better related to an amorphous material with a semi-conducting behaviour close to that of SiC.

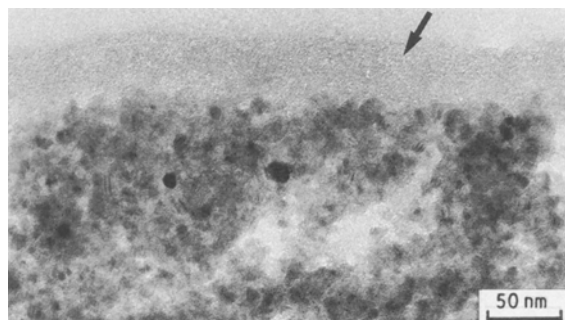


Figure 9 TEM analysis of a PCS filament stabilized with oxygen and heat treated at 1400 °C under an inert atmosphere: bright-field image.

For $T_p > 1200$ °C, e.g. for $T_p = 1400$ °C, the electrical behaviour exhibits a quasi-metallic character, i.e. it is high and almost temperature independent. The dramatic change observed in the electrical behaviour when T_p is raised above 1200 °C is obviously a consequence of the chemical and microstructural change that occurs in the PCS filaments in this temperature domain. Namely, and as already proposed by Bouillon *et al.* [26] and Monthieux *et al.* [29], the increase in conductivity which is observed for $T_p > 1200$ °C could be related to (i) the decomposition of the Si(C,O) amorphous matrix, and (ii) the formation of incomplete shells of carbon surrounding the SiC grains and which might give rise to a percolation effect [26].

3.4. Mechanical property change during PCS filament pyrolysis

The results of the tensile and torsion tests, performed at room temperature on PCS monofilaments cross-linked by oxygen and then heat treated under an inert atmosphere, are shown in Figs 14 and 15 as a function of the highest temperature, T_p , to which the material was exposed during the heat treatment. The related stiffness and failure strength data are listed in Table VI. The failure strength data were treated statistically on the basis of a two-parameter Weibull distribution. The values of the Weibull modulus, m , are given in Table VI.

Generally speaking, the stiffness moduli (i.e. E and G) as well as the ultimate tensile failure stress, σ^R , first increase with increasing T_p , then undergo maxima for $T_p = 1200$ °C and finally decrease as T_p is still increased up to 1400 °C. These experimental results are in agreement with those (for E and σ^R) reported by Yajima *et al.* [40] for ex-PCS fibres. Furthermore, the values of the stiffness moduli measured in the present work for $T_p = 1200$ °C, i.e. $E = 190$ GPa and $G = 71$ GPa are close to those given by the producer (Nippon Carbon), i.e. $E = 210$ GPa and $G = 77$ GPa for the ceramic-grade (NLM 202) Nicalon fibre thought to be produced from the same kind of PCS precursor and at a similar T_p .

Two examples of failure surface scanning electron micrographs are shown in Fig. 16. That corresponding to $T_p = 1200$ °C is typical of an amorphous brittle

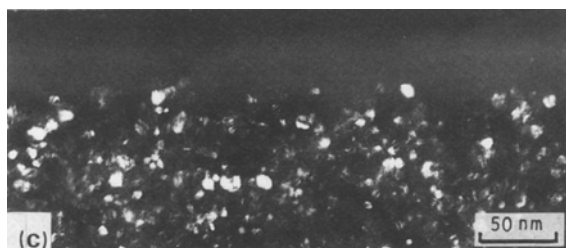
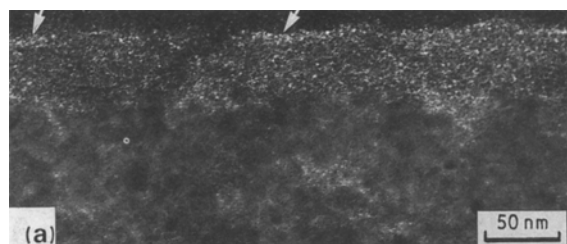


Figure 10 TEM analysis of a PCS filament stabilized with oxygen and heat treated in an inert atmosphere. Dark-field image corresponding to different locations of the aperture; (a, b) position 1 and 1 perpendicular (carbon 002), and (c) position 2 (β -SiC 111).

material, whereas that obtained for the filament heat treated at 1400°C clearly shows a polycrystalline character. This difference is further evidence of the important structural/microstructural change that occurs in ex-PCS monofilaments between 1200 and 1400°C , as discussed in the above sections.

The increase in σ^R , E and G observed when T_p is raised from 850 to 1200°C , could be related to a progressive ceramization of the material which remains amorphous (evolution of residual organic light species, e.g. CH_4 , as well as hydrogen, with an increase in density). As a result, for $T_p = 1200^\circ\text{C}$, the UTS is high and the failure surface typical of a brittle non-crystalline material. The decrease in both stiffness and failure

strength which is observed for $T_p > 1200^\circ\text{C}$ is related to the structural/microstructural change which has already been mentioned. The dramatic UTS decrease which occurs when T_p is raised from 1200 to 1400°C results directly from the crystallization of the amorphous matrix still present at 1200°C , followed by grain coarsening (both phenomena increasing the size of the defects which may initiate the failure of the filaments). The low values of the stiffness moduli, with respect to pure polycrystalline SiC, are probably due to the fact that the SiC grains are surrounded by incomplete cages of poorly ordered carbon with a low rigidity.

4. Modelling and conclusion

During the pyrolysis of a stabilized PCS filament, performed under an inert atmosphere, two important changes occur in the material: (i) an organic-inorganic transition at 500 to 750°C yielding an amorphous material which remains stable up to about 1100 to 1200°C , and (ii) above this limit, a thermal decomposition of this amorphous material resulting in the formation of a mixture of β -SiC and carbon with an evolution of gaseous species containing oxygen. These chemical, structural and microstructural changes strongly modify the physical and mechanical properties of the filament.

The organic-inorganic transition takes place within a material made of complex polymeric structural units (PSU) cross-linked through strong Si-O-Si bonds (resulting from the oxidation of the Si-H bonds present in PCS, during the stabilization step). During this transition, most organic lateral bonds are broken with an evolution of gaseous species (e.g. hydrocarbons, silanes, hydrogen, etc.) and a significant weight loss (about 10%). It yields a material which is amorphous, mainly made of silicon-based tetrahedra SiC_4 and/or $\text{SiC}_{4-x}\text{O}_x$ and already containing C-C bonds. At this stage, it is thought that the Si-C-O skeleton of the PSUs is maintained, at least in its main features.

When the amorphous filament is further heated, i.e. up to about 1100 to 1200°C , the majority of the residual organic bonds are broken with a slight additional gas evolution (e.g. of H_2 and CH_4), the material remaining amorphous. At this stage, the overall chemical formula ($\text{Si}_4\text{C}_{4.88}\text{O}_{2.12}$, where oxygen is probably slightly over-estimated) is close to $\text{Si}_4\text{C}_5\text{O}_2$ (plus trace amounts of hydrogen) and the material can be described as a continuum of SiC_4 and $\text{SiC}_{4-x}\text{O}_x$ species

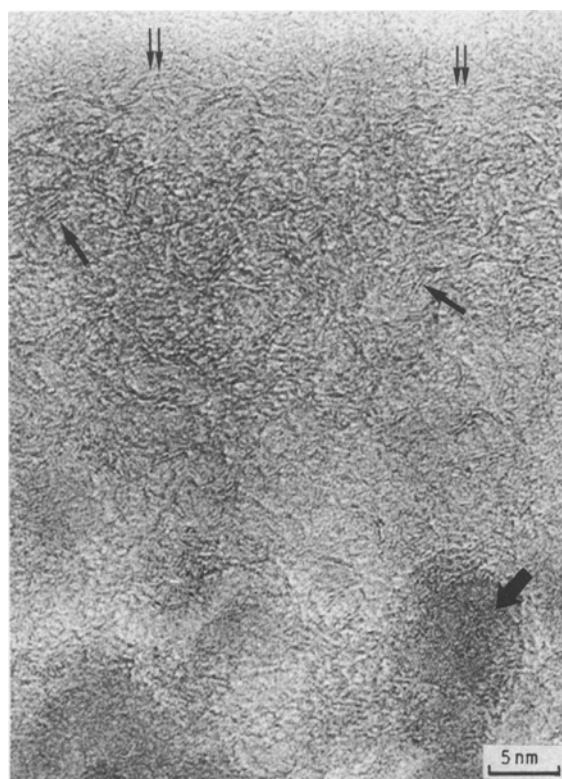


Figure 11 TEM analysis of a PCS filament stabilized with oxygen and heat treated at 1400°C under an inert atmosphere: lattice-fringe image.

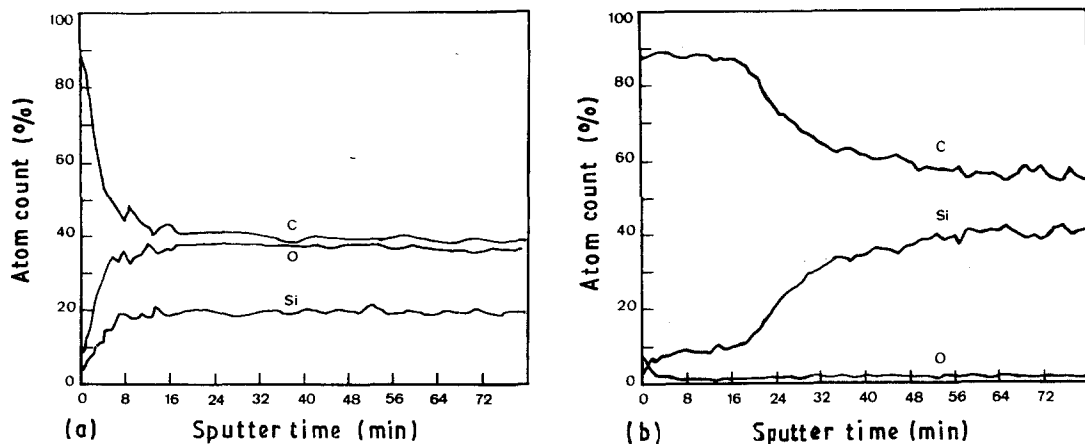


Figure 12 AES analysis (depth-profiling mode) of PCS filaments stabilized with oxygen and heat treated at increasing temperatures under an inert atmosphere at (a) 1200 °C and (b) 1400 °C.

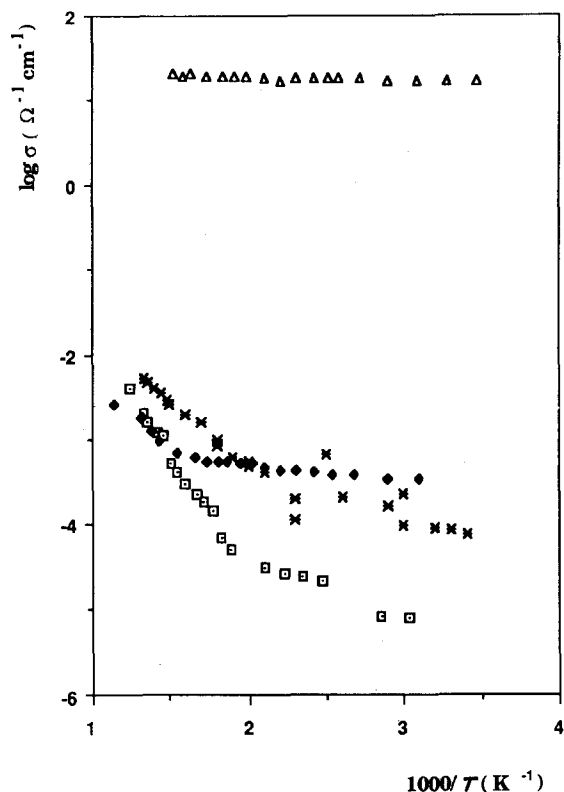
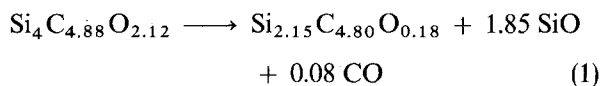


Figure 13 Thermal variations of the electrical conductivity of PCS filaments, stabilized with oxygen and heat treated at increasing temperatures under an inert atmosphere, as a function of reciprocal temperature. (□) 850 °C, (◆) 1100 °C, (*) 1200 °C, (△) 1400 °C.

which might contain, on a nanometre scale, free carbon as isolated small BSUs. As a result of this very homogeneous microstructure, such filaments exhibit a high mechanical strength and semi-conducting properties.

At still higher temperatures, i.e. for $1200 < T_p < 1400$ °C, a thermal decomposition of the amorphous continuum state occurs with a new gas evolution, a significant cross-section shrinkage (i.e. about 40%) and the formation of a mixture of carbon and SiC (mainly as the β -modification). On the basis of chemical analysis data, it is thought that the main gaseous species formed during this thermal decomposition is SiO and in lower proportion CO, in agreement with the conclusion previously drawn by Johnson *et al.*

[25] for Nicalon fibres. Therefore, the thermal decomposition could correspond to the following overall equation



with a pyrolytic residue of overall formula close to Si_2C_5 . The composition of the filaments at 1400 °C actually observed, i.e. $\text{Si}_2\text{C}_{4.4}\text{O}_{0.14}$ is close to that expected from Equation 1 and the filaments consist of a mixture of SiC and carbon almost free of oxygen. Furthermore, Equation 1 should yield a weight loss of 43% which is in rather fair agreement with the important shrinkage of the fibre diameter (from about 16 μm to about 13 μm corresponding to a weight loss of 34%).

From Equation 1, one could expect (i) an important weight loss as already mentioned, (ii) the formation of free carbon, and (iii) a large and rapid growth of silicon carbide crystals (because the nanodomains of SiC which are thought to be isolated from each other by BSUs of carbon and the oxygen-rich phase, according to the model of Laffon *et al.* [16] can now grow freely). This is what has actually been observed. At last, the partial degradation of carbon BSUs surrounding SiC crystals can be explained on the basis of the oxidation of carbon by SiO species according to the following equation



The drop in the filament failure strength occurring at 1200 to 1400 °C is a direct consequence of the amorphous-crystalline state transition. Similarly, the dramatic increase observed in the electrical conductivity (i.e. of four orders of magnitude) associated with a semi-conductor-quasi-metal transition could be due to a percolation phenomenon related to the formation of the network of carbon at the SiC grain boundaries. Finally, the low stiffness of the filaments, and more generally speaking of ex-PCS fibres (i.e. $E = 200$ GPa instead of 450 GPa for polycrystalline SiC) could be related to the fact that the filament is not made of pure SiC but consists of a mixture of SiC and carbon of low stiffness.

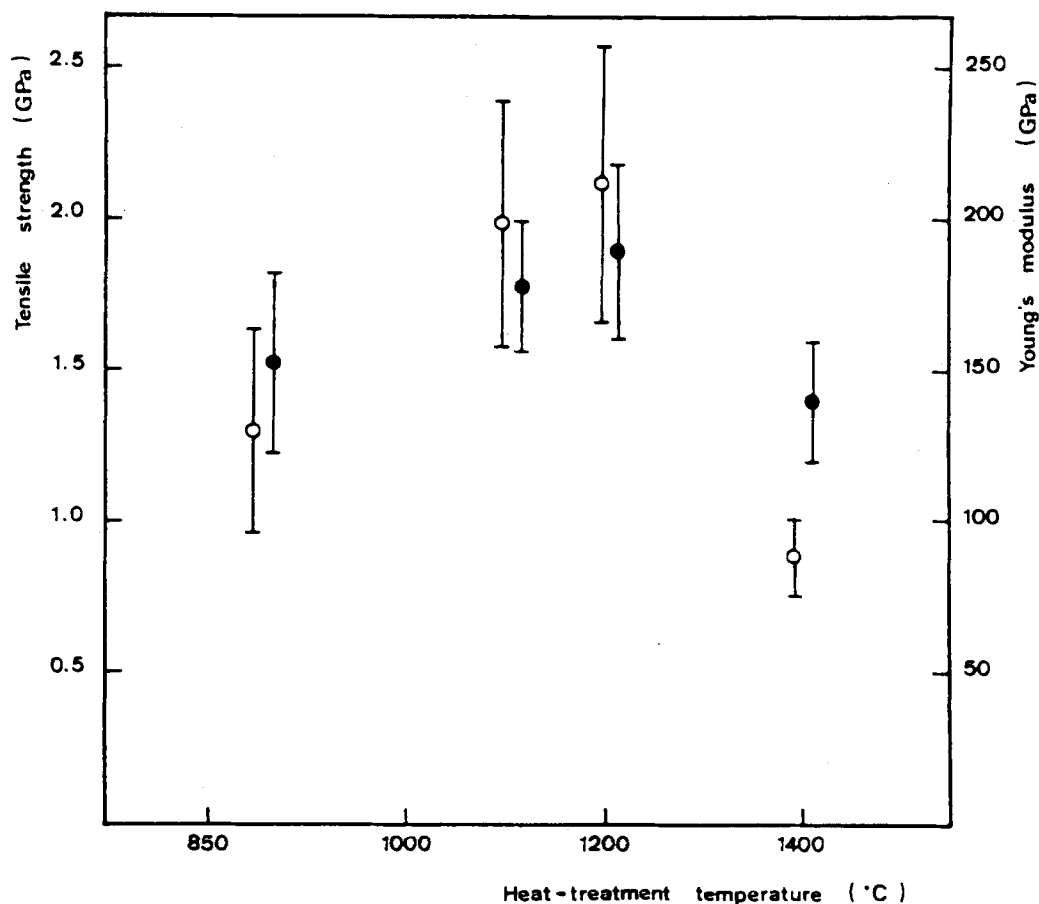


Figure 14 Thermal variations of the (○) UTS and (●) Young's modulus measured at room temperature, of ex-PCS monofilaments as a function of the pyrolysis temperature, T_p . An average of 40 samples (gauge length 10 mm) was tested for each T_p value.

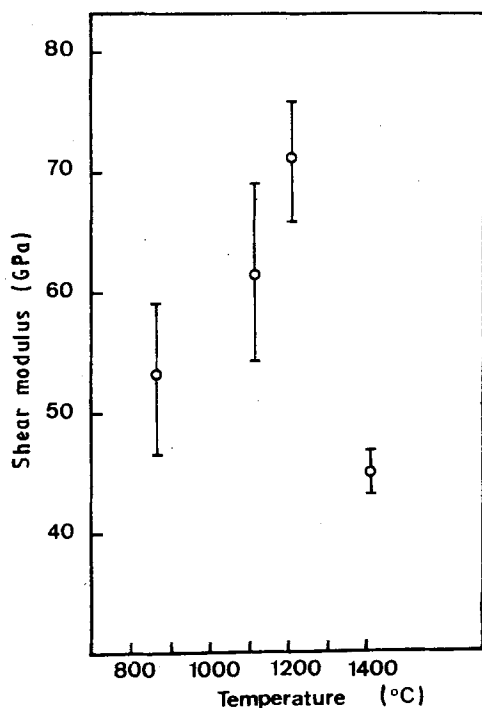


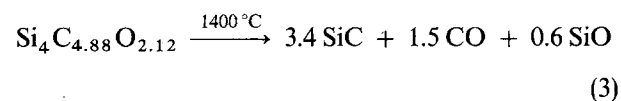
Figure 15 Variations of the shear modulus, measured at room temperature in torsion, of ex-PCS monofilaments as a function of the pyrolysis temperature. An average of ten samples was tested for each T_p value.

A preliminary thermodynamic study, based on the minimization of the total Gibbs free energy of the system, has been performed [44] in order to assess (i) the nature of the chemical species present in the gas

phase and in the solid, as well as (ii) the ratio of the partial pressures of CO and SiO, when equilibrium is achieved at a given temperature and within an isothermal vessel of given volume, for an overall chemical composition corresponding to that of our pyrolytic residue at 1100 to 1200 °C, i.e. $\text{Si}_4\text{C}_{4.88}\text{O}_{2.12}$.

From the results of the calculations, shown in Table VII it appears that the solid corresponding to $\text{Si}_4\text{C}_{4.88}\text{O}_{2.12}$ should be at 1200 °C, a mixture of SiC, silica and free carbon, assuming that equilibrium is reached within a vessel of small volume, CO being the main gaseous species. It is worthy of note that this result is consistent with surface AES analyses reported by Menessier [45] for Nicalon fibres annealed in sealed silica tubes at a somewhat lower temperature.

When both the temperature and the volume of the vessel are increased (in the calculations, a vessel of very large volume being close to an open system configuration), (i) the proportion of SiO with respect to that of CO becomes much more important, and (ii) the solid consists of pure silicon carbide only. Under such conditions, the following overall equation can be written



which should be compared to Equation 1. On the one hand, the evolution of SiO, during the pyrolysis at 1400 °C of the ex-PCS residue, has been established indirectly in the present study from chemical analyses

TABLE VI Stiffness moduli and UTS of ex-PCS monofilaments, measured at room temperature, for increasing pyrolysis temperatures ($\sigma_{rel.}^R$, $E_{rel.}$ and $G_{rel.}$ are normalized values calculated taking the data obtained at 1200 °C as references)

Temperature of pyrolysis T_p (°C)	Ultimate tensile failure stress			Young's modulus		Shear modulus	
	σ^R (MPa)	$\sigma_{rel.}^R$ (%)	m	E (GPa)	$E_{rel.}$ (%)	G (GPa)	$G_{rel.}$ (%)
850	1300	61	4	155	82	54	75
1100	1990	94	5	180	95	61	86
1200	2120	100	5	190	100	71	100
1400	880	42	6	140	74	45	63

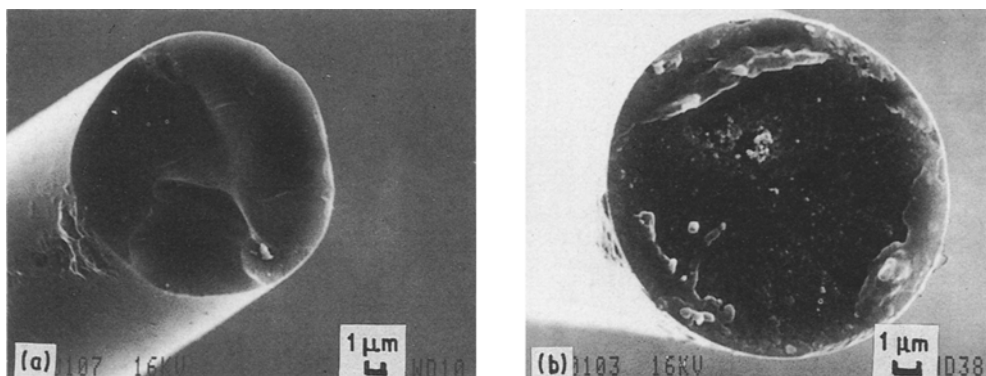


Figure 16 Failure surface of ex-PCS monofilaments, loaded in tension and tested at room temperature, as a function of the pyrolysis temperature: (a) $T_p = 1200$ °C, (b) $T_p = 1400$ °C.

TABLE VII Nature of solid phases and gaseous species, and the partial pressures of CO and SiO at equilibrium, for a system of overall chemical formula $Si_4C_{4.88}O_{2.12}$ as a function of temperature and volume of the gas phase

Volume (l)	Temperature (°C)	P_{CO}/P_{SiO}	Phases in the solid state	Phases in the gas phase
1	1200	572	SiC-SiO ₂ -C	CO-(SiO)
1	1400	266	SiC-SiO ₂ -C	CO-(SiO)
1000	1400	17	SiC-SiO ₂	CO-SiO
100000	1400	2.5	SiC	CO-SiO

of the solid. It has been also directly evinced experimentally by Johnson *et al.* [25], as already mentioned. On the other hand, the fact, that the residue actually obtained at 1400 °C does not consist of pure SiC but of a SiC + C mixture, could be explained on the basis of (i) the thermodynamic approach does not take into account the kinetics factors, and (ii) the experimental vessel actually used was not isothermal; therefore, the decomposition of SiO (into SiO₂ and silicon) on the cold wall shifts Reaction 2 towards the left-hand side and may favour the formation of free carbon.

Several points still remain a matter of speculation, in particular the origin of the carbon layer at the filament surface, for $T_p > 1200$ °C. Such a carbon layer, mentioned already by several authors, is partly responsible for the high toughness of CMCs made of ex-PCS fibres and prepared at high temperatures (e.g. by CVI or hot pressing). The majority of this carbon layer is made of randomly orientated BSUs and furthermore, there exists a composition gradient between this layer of almost pure carbon and the SiC + C filament, which suggests a decomposition process governed by diffusion (possibly activated by the SiO

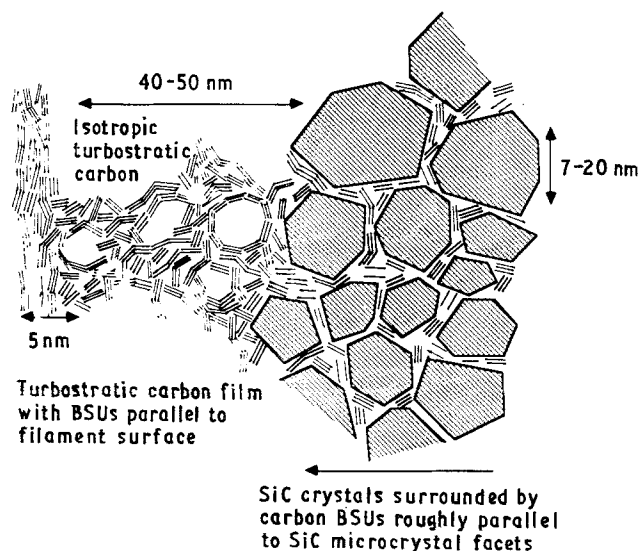


Figure 17 Schematic microstructure of ex-PCS filaments heat treated at 1400 °C under an inert atmosphere, in the vicinity of the filament surface.

gaseous species). Finally, the very thin films of turbostratic carbon, whose layers are parallel to the filament surface, could be the result of a CVD reaction from the residual gaseous carbosilane species present in the atmosphere of the pyrolysis furnace. Obviously, additional research would be necessary in order to confirm the origin of this very important carbon layer formed at the ex-PCS filament surface during annealing treatments. A model of the filament microstructure is tentatively shown in Fig. 17.

Acknowledgements

The authors acknowledge the contribution of P. Dordor to the electrical study of the filaments as

well as M. Loubinou and P. Olry, ITF and SEP, respectively, for their assistance in setting up the monofilament extrusion apparatus. They are indebted to UA 35 for the supply of modified PCS starting material and to B. Cheynet from THERMODATA for the thermodynamic calculations. This work was supported by AFME and SEP (grant to E. Bouillon) as well as CNRS, DRET and Conseil Régional d'Aquitaine.

References

1. R. NASLAIN, "Introduction to Composite Materials", Vol. 2, "Metallic and Ceramic Matrix Composites" (in French) (CNRS/IMC, Bordeaux, 1985).
2. S. YAJIMA, in "Handbook of Composites", Vol. 1, edited by W. Watt and B. V. Perov (Elsevier, Amsterdam, 1985).
3. S. YAJIMA, J. HAYASHI and M. OMORI, *Chem. Lett.* (1975) 931.
4. S. YAJIMA, K. OKAMURA and M. OMORI, *ibid.* (1975) 1209.
5. S. YAJIMA, Y. HASEGAWA, J. HAYASHI and M. IIMURA, *J. Mater. Sci.* **13** (1978) 2529.
6. Y. HASEGAWA, M. IIMURA and S. YAJIMA, *ibid.* **15** (1980) 720.
7. Y. HASEGAWA and K. OKAMURA, *ibid.* **18** (1983) 3633.
8. *Idem*, *ibid.* **21** (1986) 321.
9. K. OKAMURA, *Composites* **18** (1987) 107.
10. K. OKAMURA, US Pat. 4 650 773 17 (1987).
11. K. OKAMURA, M. SATO, Y. HASEGAWA and T. AMANO, *Chem. Lett.* (1984) 2059.
12. L. C. SAWYER, M. JAMIESON, O. BRIKOWSKI, M. I. HAIDER and R. T. CHEN, *J. Amer. Ceram. Soc.* **70** (1987) 798.
13. Y. MANIETTE and A. OBERLIN, *J. Mater. Sci.* **24** (1989) 3361.
14. J. LIPOWITZ, H. A. FREEMAN, R. T. CHEN and E. R. PRACK, *Adv. Ceram. Mater.* **2** (1987) 121.
15. L. C. SAWYER, R. T. CHEN, F. HAIMBACK, P. J. HARGET, E. R. PRACK and M. JAFFE, *Ceram. Engng Sci. Proc.* **7** (1986) 914.
16. C. LAFFON, A. M. FLANK, R. HAGEGE, P. OLYR, J. COTTERET, M. LARIDJANI, J. DIXMIER, J. L. MIQUEL, H. HOMMEL and A. P. LEGRAND, *J. Mater. Sci.* **24** (1989) 1503.
17. T. J. CLARK, R. M. ARONS, J. B. STAMMATOFF and J. RABE, *Ceram. Engng Sci. Proc.* **7-8** (1985) 576.
18. A. S. FAREED, P. FONG, M. J. KOCZAK and F. M. KO, *Amer. Ceram. Soc. Bull.* **66** (1987) 353.
19. T. MAH, N. L. HEICHT, D. E. McCALLUM, J. R. HOENIGMAN, H. M. KIM, A. P. KATZ and H. A. LIPSITT, *J. Mater. Sci.* **19** (1984) 1191.
20. L. C. SAWYER, R. ARONS, F. HAIMBACK, M. JAFFE and K. D. RAPPAPORT, *Ceram. Engng Sci. Proc.* **7-8** (1985) 567.
21. G. SIMON and A. R. BUNSELL, *J. Mater. Sci.* **19** (1984) 3649.
22. T. J. CLARK, M. JAFFE, J. RABE and N. R. LANGLEY, *Ceram. Engng Sci. Proc.* **7-8** (1986) 901.
23. Y. SASAKI, Y. NISHIMA, M. SATO and K. OKAMURA, *J. Mater. Sci.* **22** (1987) 443.
24. K. L. LUTHRA, *J. Amer. Ceram. Soc.* **69** (1986) C-231.
25. S. M. JOHNSON, R. D. BRITAIN, R. H. LAMOREAUX and D. J. RAWCLIFFE, *ibid.* **71** (1988) C-132.
26. E. BOUILLON, F. LANGLAIS, R. PAILLER, R. NASLAIN, J. C. SARTHOU, A. DELPUECH, C. LAFFON, P. LAGARDE, F. CRUEGE, P. V. HUONG, M. MONTHIOUX and A. OBERLIN, *J. Mater. Sci.* in press.
27. E. BOUILLON, R. PAILLER, R. NASLAIN, E. BACQUE, J. P. PILLOT, M. BIROT, J. DUNOGUES and P. V. HUONG, *ibid.*
28. A. OBERLIN, *Carbon* **17** (1979) 7.
29. M. MONTHIOUX, A. OBERLIN and E. BOUILLON, *Compos. Sci. Technol.* **37** (1990) 21.
30. A. R. BUNSELL, J. W. S. HEARLE and R. D. HUTER, *J. Phys. E. Sci. Instrum.* **4** (1971) 868.
31. J. F. VILLENEUVE, Internal report (1988) LCTS (UM47) 33600 Pessac, France.
32. J. J. POUPEAU, D. ABBE and J. JAMET, ONERA Report (1982).
33. L. PORTE and A. SARTRE, *J. Mater. Sci.* **24** (1989) 271.
34. J. A. TAYLOR, *Appl. Surf. Sci.* **7** (1981) 168.
35. Y. MIZOKAWA, K. M. GEIB and C. W. WILMSEN, *J. Vac. Technol. A.* **4** (1986) 1696.
36. M. N. RAHAMAN and L. C. DE JONGHE, *Amer. Ceram. Soc. Bull.* **66** (1987) 782.
37. T. GOTO, F. ITOH, K. SUZUKI and T. HURUI, *J. Mater. Sci. Lett.* **2** (1983) 805.
38. W. Y. LEE, *J. Appl. Phys.* **51** (1980) 3365.
39. R. PAMPUCH, W. PTAK, S. JONA and J. STOCH, in "Energy and Ceramics", edited by P. Vincuzini (Elsevier, Amsterdam, 1980) pp. 435-48.
40. S. YAJIMA, K. OKAMURA, T. MATSUZAWA and T. SCHISHIDO, *Nature* **279** (1979) 706.
41. A. OBERLIN, *Carbon* **22** (1984) 521.
42. A. OBERLIN, S. BONNAMY, X. BOURRAT, M. MONTHIOUX and J. N. ROUZAUD, *ACS. Symp. Ser.* **303** (1986) 85.
43. P. LECOUSTUMER, M. MONTHIOUX and A. OBERLIN, in "Composite Materials for High Temperature Applications" (in French), edited by P. Naslain, J. Lamalle and J. L. Zulian (Amac-Codemac, Bordeaux, 1990).
44. Thermodata, Saint-Martin d'Hères (1988).
45. E. MENESSIER, University thesis 216, Bordeaux (1988).

Received 4 August 1989
and accepted 19 February 1990